



A laser-based system to heat nuclear fuel pellets at high temperature

C. Cifuentes Quintal, M. Reymond, F. Fiorito, F. Martin, M. Pontillon, J. Richaud, T. Doualle, Y. Pontillon, L. Gallais

► To cite this version:

C. Cifuentes Quintal, M. Reymond, F. Fiorito, F. Martin, M. Pontillon, et al.. A laser-based system to heat nuclear fuel pellets at high temperature. *Review of Scientific Instruments*, 2023, 94 (10), 10.1063/5.0139508 . hal-04453724

HAL Id: hal-04453724

<https://cnrs.hal.science/hal-04453724>

Submitted on 14 Feb 2024

HAL is a multi-disciplinary open access archive for the deposit and dissemination of scientific research documents, whether they are published or not. The documents may come from teaching and research institutions in France or abroad, or from public or private research centers.

L'archive ouverte pluridisciplinaire **HAL**, est destinée au dépôt et à la diffusion de documents scientifiques de niveau recherche, publiés ou non, émanant des établissements d'enseignement et de recherche français ou étrangers, des laboratoires publics ou privés.

A laser-based system to heat nuclear fuel pellets at high temperature

C. Cifuentes Quintal^{1,2}, M. Reymond^{1,2}, F. Fiorito¹, F. Martin¹, M. Pontillon¹, J.C. Richaud¹, T. Doualle¹, Y. Pontillon^{1,*}, L. Gallais²

¹CEA, DES, IRESNE, DEC, Cadarache F-13108 Saint-Paul-Lez-Durance, France

²Aix Marseille Univ, CNRS, Centrale Marseille, Institut Fresnel, Marseille, France

*The authors to whom correspondence may be addressed: yves.pontillon@cea.fr, laurent.gallais@fresnel.fr

Abstract

Annealing tests are of utmost importance in nuclear fuel research particularly to study thermophysical properties of the material, microstructure evolution or the released gas as a function of temperature. As an alternative to conventional furnace or induction annealing, we report on a laser-heating experiment allowing one to heat a nuclear fuel pellet made of uranium dioxide, UO_2 , or potentially other nuclear fuel pellet in an isothermal and controlled manner. For that purpose, we propose to use an indirect heating method based on a two compartment tungsten crucible, one containing the sample and the other one acting as a laser susceptor for efficient and homogeneous heating of the assembly. With this concept we demonstrate the heating of UO_2 samples up to 1500°C at a maximum heating rate of 30°C/s with the use of two 500 W lasers. The system is however scalable to higher heating rates or higher temperatures by increasing the laser power up to few kW. The experiment has been designed to heat a Pressurized Water Reactor fuel pellet, but the concept could be easily applied to other sample geometries or materials.

I. Introduction

Experimental data allowing for an accurate qualification of nuclear fuel together with quantification of its behavior under both nominal or hypothetical accidental conditions is of crucial importance in the nuclear industry. For instance, predicting accurately the Fission Gas Release (FGR) from high burn up UO_2 and/or MOX (Mixed Oxide) fuels at off-normal conditions is a significant and important challenge. Usual studies in this field require dedicated annealing tests in order to monitor both the absolute level and the time dependence of the released gas. In this context an annealing device, referred as MERARG (French acronym for Means of Study for Annealing and Gaseous Release Analysis) (Menegon et al., 2008; Pontillon et al., 2009; Noirot et al., 2014), has been developed to study the behavior of nuclear fuel under thermal transient representative of Loss of Coolant Accident (LOCA). It allows annealing at high temperature, usually between 1200°C and 1600°C but can reach peak of 2800°C , on irradiated nuclear fuel pellets with slow (between 0.05 and 0.5°C/s) and moderate (maximum $20\text{--}30^\circ\text{C/s}$) temperature ramps thanks to an induction furnace. This device is coupled both with dedicated analysis loops - that are designed to identify and quantify the gaseous fission products released during the annealing sequence-, and extensive ex-situ microstructure characterization technics (i.e. SEM, TEM, EPMA, SIMS) of the annealed fuel sample. Recently we have upgraded MERARG with an imaging system for the real time monitoring of the sample surface to provide additional information on the microstructure evolution and possible fragmentation during the annealing tests. This optical system is also coupled with non-contact temperature measurements by thermal radiation analysis to monitor and control the fuel temperature (Vidal et al, 2020).

To study other types of hypothetical accidentals sequences such as Reactivity Initiated Accident (RIA), a laser-based platform is currently being developed at CEA to perform specific annealing tests on nuclear fuels (Vidal et al, 2020 ; Reymond et al, 2021). In this context it is interesting to build on MERARG's concept by proposing an analogous experiment using lasers to reach similar performances and possibly to surpass current limitations. The perspective of our work is to propose a single laser platform able to investigate nuclear fuel behavior under various conditions, by using the flexibility of

the laser heating technique. Indeed, the management of out-of-pile experiments on irradiated fuels in a “hot-laboratory” environment is often challenging and developing a unique and flexible platform is important both from a scientific and from an operating point of view.

The main advantage of the laser-heating technique is the ability to deliver large amounts of energy at high rates, thus allowing one to reach high heating rates. It is also a contactless technique providing and facilitating the implementation of the surrounding instrumentation. Moreover, the beam characteristics (wavelength, beam size, temporal and spatial shape, exposure time, power) are highly configurable and, as a consequence, can be finely adjusted for a specific target process. Because of these advantages, laser techniques have been successfully applied for heating in different studies related to nuclear fuels studies: direct laser surface heating for melting point measurement (Manara et al, 2008), laser heated furnace for Knudsen cell mass spectrometry (Colle et al, 2008), laser heating and melting in aerodynamic levitation (Weber et al, 2016) or laser-induced thermos-desorption (Horlait et al, 2021) to give some examples.

In this paper, we report on a laser-heating experiment allowing one to heat a PWR (pressurized water reactor) nuclear fuel pellet in an isothermal and controlled manner. Various concepts and configurations have first been taken into account and the retained one, on the basis of thermal and optical simulations, is detailed in the first part of the paper. The approach is quite similar to the one presented in (Colle et al, 2008), but with specificities based on MERARG’s concept, and the objective to be used to heat fuel pellets. Moreover, our system is compatible with specific instruments that were specifically designed for MERARG (Vidal et al, 2020). We will present the experimental developments that have been conducted on the CHAUCOLASE (French acronym for Controlled Laser based heating) platform, a high power laser facility to conduct annealing tests at high temperature, previously presented in (Minissale et al, 2020). Finally, as a proof of concept, we conducted a heating experiment with depleted UO_2 fuel pellets that we submitted to a typical thermal sequence of interest.

II. Concept and General Design

The objective of the laser heating device is to heat a nuclear ceramic cylinder made of uranium dioxide, UO_2 , or potentially other nuclear fuels (Mixed OXide (MOX) for instance), of around 8 mm of diameter and 13.5 mm high. The heating should be as homogenous as possible within the sample, minimizing thermal gradients in order to avoid thermal stresses inside that can cause for example fractures in the fuel. In addition, from a general point of view, the temperature ramps applied thanks to MERARG cover a range from 0.05°C/s to $30\text{-}40^\circ\text{C/s}$ for target temperatures between 800°C and 1500°C . These parameters make it possible to cover the majority of thermal sequences representative of the incident situations studied with this device. However, most of the studies (i.e. for the study of LOCAs) focus on the couple 20°C/s - 1200°C

Two alternative configurations have been considered before choosing the retained one (figure 1): a) Illuminating directly the pellet on its whole circumference, UO_2 being a strongly absorbing material at the used wavelength ; b) Illuminating directly a crucible containing the pellet.

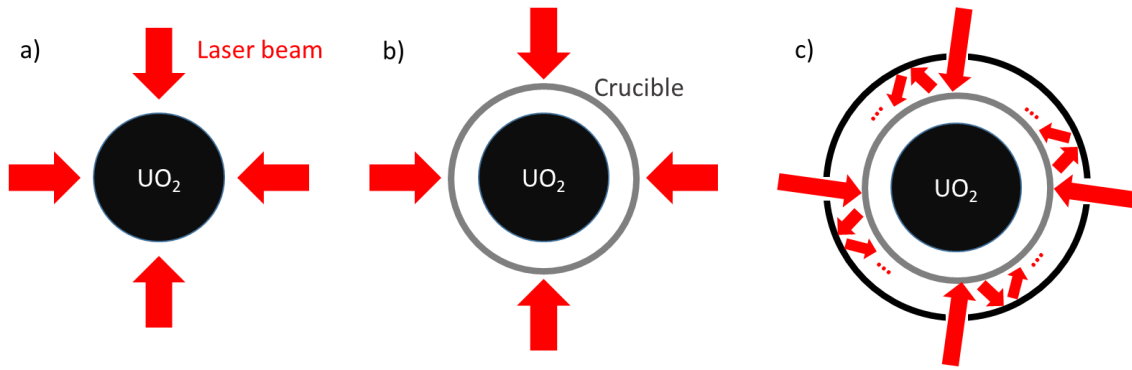


Figure 1: Top view of two of the three considered configurations. The number of laser beamlets is not restricted to 4. a) Illuminating directly the pellet. b) Illuminating directly a crucible containing the pellet. c) Confining the laser beam between two metallic walls. A part of the laser power is absorbed at each reflection on the metallic surfaces.

Despite their simplicity, the weaknesses of these direct approaches are limiting their applicability. Illuminating the pellet on its whole circumference in a homogeneous way is tedious and would require the use of four or more beamlets, more beams meaning a better homogeneity of the induced thermal loading but more experimental complexity. Alternatively, diverging beams covering the pellet diameter could be used, but still with experimental complexity. Moreover, the integrity of the pellet in these thermal sequences is not assured as cracking and fragmentation is expected. As such, illuminating directly the pellet cannot be considered. Illuminating directly a crucible would ensure a more homogeneous heating of the pellet by radiative and conductive heat exchanges from the crucible to the sample. The issue of homogeneity remains however the same as the crucible must be heated in the most homogenous way possible if one wants to heat the sample inside homogeneously as well, leading to the use of four or more beams. Moreover, the crucibles typically used are made either of tungsten, platinum or molybdenum which are metals and are as such have highly reflective surfaces. This would lead to important loss of laser power as it will be showed later, an important amount of it being simply reflected instead of being absorbed.

For all these reasons, the third envisioned configuration consists in c) confining the laser beam between a metallic crucible and a second metallic wall that we will hereinafter call hood (Figure 1.c). The beam is injected in this system through a small opening cut in this second wall. The beam is thus confined and absorbed through multiple reflections between the internal crucible and the hood, ensuring that almost all of the laser intensity is absorbed by the system, a small fraction being obviously lost by reflection through the opening in the hood. This configuration is interesting because the power absorbed by the hood would then contribute to the heating of the sample by radiative heating of the crucible and as such it limits power losses due to optical reflections. However a part of the power is lost by thermal radiation from the external surfaces of the hood. To ensure homogeneous heating of this system, the laser beam must be roughly the same height as the crucible and in order to minimize the losses through the openings, it must be as thin as possible. Therefore, our laser beam must have the shape of a thin laser line. This configuration is further explored in the simulations in the next section. Let's note also that an alternative solution would have been a crucible, as in b), with holes for injection of the laser inside the crucible, it was however not retained because of possible uncontrolled heating of some parts of the sample that could lead to vaporization.

III. Simulations

III.a. Thermal simulations

We have conducted series of thermal simulations to ensure the validity of our approach and to have a first evaluation of the laser power needed. To do so, the pellet-crucible system has firstly been modeled in a Finite Element simulation software (COMSOL Multiphysics) in a 2D axisymmetric geometry (see Figure 2). The crucible material is Tungsten, and we have used the thermal properties recommended in (Davis et al, 1996) for the simulations. The crucible geometry and dimensions corresponds to the one currently in used on the MERARG facility. The thermal properties of UO_2 were taken from (Fink, 1999). We have considered heat conduction inside the crucible and the pellet, with perfect heat contact between the two materials. Radiative heat exchange inside the crucible is considered, as radiative heat losses towards ambient from the external wall of the crucible. Convection is however not taken into account in the simulations because the experiments have been conducted in vacuum. At this point the laser deposited power is considered as a homogeneous incoming heat flux on the external cylindrical surface of the crucible. The optical aspects will be considered in the next section. We have taken into account a ratio of absorbed power to incident power of 0.3, which is the order of magnitude at $1\text{ }\mu\text{m}$ wavelength (Minissale et al, 2017), as such for a considered laser flux of 1000 W, only 300 W of heat flux is applied on the crucible (we will refer to 'laser flux' and 'heat flux' in the following).

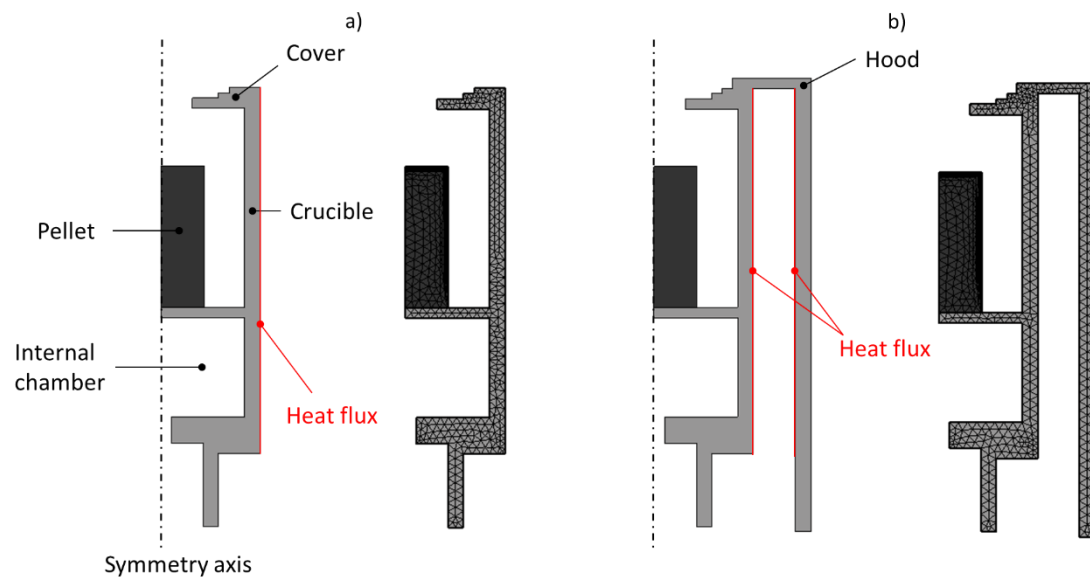


Figure 2: Schematic and meshing of the crucible assembly and UO_2 pellet. **a)** Configuration with direct heating of the crucible only. **b)** Configuration with the crucible / hood assembly and internal heating due to laser confinement. The pellet is placed inside by removing the cover part.

For a first estimation of the required laser power and thermal gradients in the pellet, we have conducted simulations with the experimental configuration displayed in Figure 2.a corresponding to direct illumination of the crucible. On Figure 3 we report on the pellet core temperature in case of a laser heat flux ranging from 100 to 1000 W, for an exposure time up to 10 minutes. As showed on this figure, with a laser flux of 1000 W, corresponding to a heat flux of 300 W, we reach a temperature plateau close to $1400\text{ }^\circ\text{C}$ with approximately a $12\text{ }^\circ\text{C/s}$ ramping speed. As shown also on Figure 3, there is a temperature gradient in the pellet, which corresponds to $\pm 50\text{ }^\circ\text{C}$ from the center temperature. These simulations showed that it should be possible in this simple configuration to reach the required temperature range of interest with a reasonable laser power considering the state-of-the-art of industrial lasers. This comes at the cost of losing 70% of the incident power, that would represent a safety hazard in addition to not being efficient. To speed-up the temperature increase, a higher laser

power would be required, with more lost power to manage. These simulations confirmed the need of a second metallic wall to confine laser power both from a practical and safety point of view.

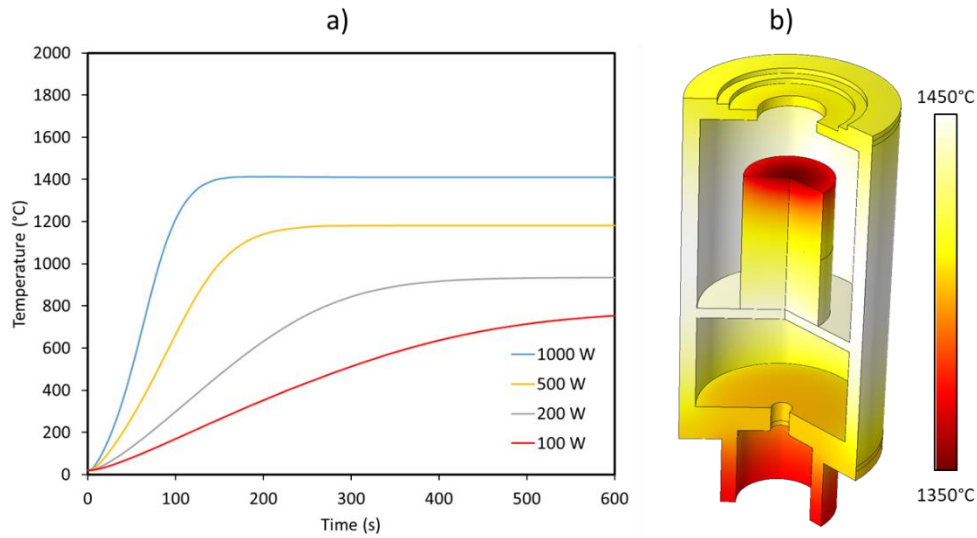


Figure 3: (a) Temperature evolution at the center of the pellet as a function of time for various laser power ; (b) Temperature distribution in the pellet/crucible assembly after reaching the steady state regime for 1000 W.

We now consider the complete system, as showed in Figure 2.b. In this 2D axisymmetric simulation, the openings in the hood are not considered. The simulation conditions are the same as previously described, with the exception that the heat source is now located on the external surface of the crucible and internal surface of the hood, as described in Figure 2.b, and that it is fully absorbed in the cavity. As such for a laser flux of 1000 W, a heat flux of 500 W is applied on both each of the two walls. This choice is arbitrary at this point but based on the fact that there are multiple reflection and scattering of the beams inside the cavity. The optical simulations described below will refine this assumption.

The simulation results are presented in Figure 4. More than 1600°C can be reached with 1000 W of total power and 1400°C for 500 W, which is half the power required without the hood. 1400°C can also be reached with a heating rate of 20°C/s from our simulations. This confirms that the approach allows us to reach temperature and ramping speed of interest while keeping the used laser power as low as possible, and ensuring the safety of experimental conditions.

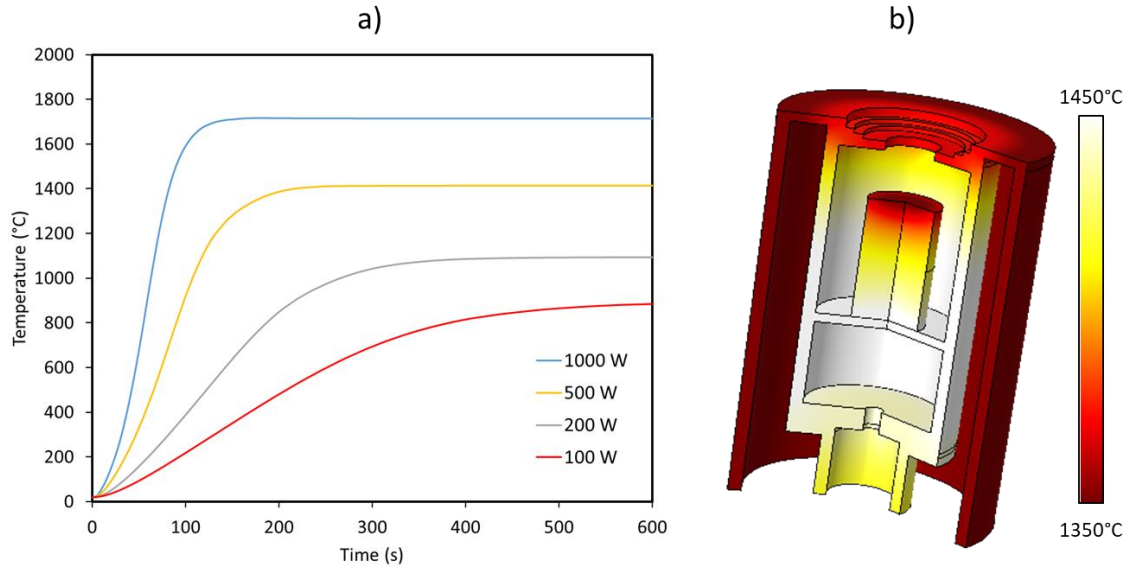


Figure 4: (a) Temperature evolution at the center of the pellet as a function of time for various laser power ; (b) Temperature distribution in the pellet/crucible/hood assembly after reaching the steady state regime for 500 W of laser power.

III.b. Optical simulations

Having discussed the configuration and studied the required laser power, we now proceed to define the optical configuration. For that purpose, we have used an optical ray tracing approach, under the COMSOL software, that is coupled to heat transfer simulations, the rays being used to defined the heat sources on the incident surfaces and the amount of transported power. We have considered as the starting point, the characteristics of available laser sources: Gaussian distribution of intensity, with radial symmetry and a beam diameter of 6.5mm (defined at $1/e^2$). To shape the beam into a line adapted to its insertion in the hood, we have used a combination of a plano-convex cylindrical divergent lens in one plane and one plano-convave cylindrical convergent lens in another plane. The first lens is used to focus the beam in the thin slit aperture of the hood, while the second lens enlarges the beam to cover the height of the crucible (see figure 5). Their focal lengths have been chosen as 200 mm and -50 mm respectively, based on geometrical optics consideration and standard lenses available.

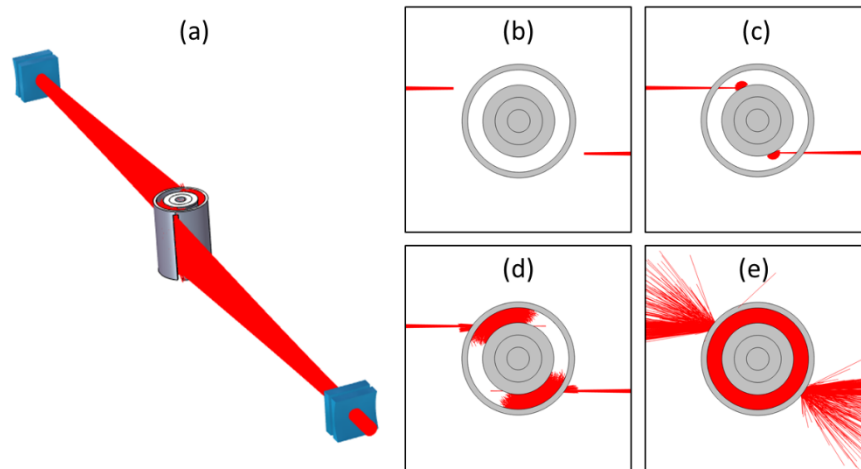


Figure 5: Ray tracing simulation of the laser heating system. (a) two optical systems based on cylindrical lenses are used to shape the gaussian beam in a thin line at the entrance of the hood/crucible assembly. (b), (c), (d), (e) top view of hood/crucible assembly. After passing through the opening, the rays are absorbed and scattered on the tungsten surfaces.

As a compromise between heating homogeneity and simplicity we have chosen a hood with two slit openings. The laser beam is injected as described in figure 5 so that it is incident at a glazing angle on the crucible to avoid back reflection through the slits. By considering the reflectance of the crucible and of the hood and its nature (diffuse or specular), we can calculate the resulting intensity distribution in the crucible-hood interstice induced by the numerous reflection and absorption between the two walls. This intensity distribution across the mesh can then be used as a heat source for thermal simulations. Different parametric studies have been conducted on the effect of hood diameter and thickness, position and width of the slits, surface quality (polished with specular reflection or rough finish with diffuse reflection) to quantify the impact of such parameters on the thermal response and the sensitivity associated with each of these parameters. This has led to experimental configuration that is described in the next section.

IV. Experiments

IV.a. Crucible assembly

The hood and crucible parts previously described have been produced in Tungsten (Figure 6). The slits have 3 mm width and 40 mm height. The surface has a rough finish with a surface roughness measured in the range 300-400 nm (root mean square height). Consequently, there is no specular reflection in the visible and near infrared. We have measured a diffuse reflectivity of 64% at 1 μm wavelength, using a home-made system based on a supercontinuum laser source, an integrating sphere and an array spectrometer. This value is in line with reported values of Tungsten in the literature (Minissale et al, 2017).

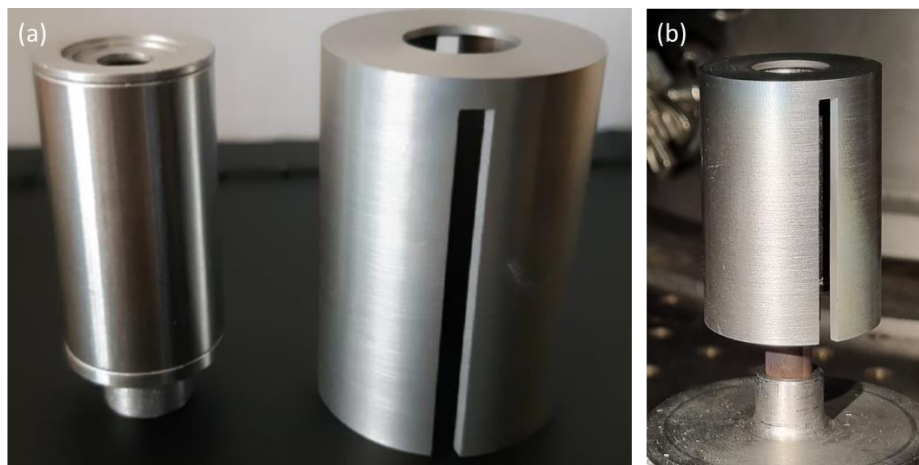


Figure 6: The hood/crucible tungsten assembly. (a) the main crucible is on the left with the crucible cover. On the right is the hood with one slit opening visible. (b) The assembly on its ceramic post.

The high temperature interaction between the tungsten crucible and the UO_2 can possibly hinder the quality of the current heat treatments. The non-oxidation of the metal crucible during the experiments is systematically checked thanks to the surface condition of the latter, which retains its original shape and surface aspect. It does not show, moreover, any trace of upper oxide of W of blue or orange color. This point is also confirmed by the feedback from more than 25 years of use of the MERARG furnace in a high activity cell (Ravel et al, 2000).

IV.b. Experimental configuration

Experiments have been conducted on the CHAUCOLASE facility, a modular platform develop and shared between CEA and Institut Fresnel which is dedicated to develop and qualify laser heating

techniques to study materials at high temperature (Minissale et al, 2020 ; Vidal et al, 2020 ; Gallais et al, 2021). For the experiments described in this paper we have used a high power CW ytterbium fiber laser (SPI laser Qube 1500), which can deliver 1500 W of maximum power with a monomode laser beam and with a typical rising time of few microseconds. The main beam is splitted into two beamlets with a 50/50 beamsplitter and directed with high reflective mirrors. After passing through the lenses that have been described previously, the beams are sent through laser windows in a vacuum chamber with a base pressure of 2×10^{-2} mbar. The crucible and hood assembly is placed at the center of the experimental chamber, mounted on a ceramic sample holder. The schematic of the experiment is described on Figure 7.

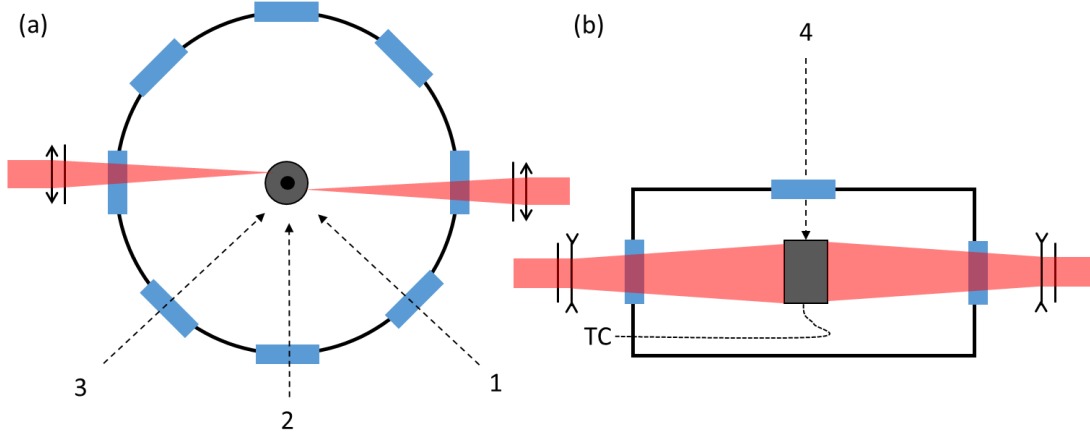


Figure 7: Schematic of the experimental set-up. (a) Top view of the experimental chamber equipped with viewports. (b) side-view of the chamber. The hood/crucible assembly is placed at the center of the chamber. The laser beam path is shown in red. 1, 2, 3 and 4 are different lines of sight for the optical instrumentation, that are referred to in the manuscript. TC corresponds to the thermocouple used for temperature monitoring of the crucible.

The chamber is equipped with lateral viewports that have been used for observation or temperature monitoring through different lines of sight that are numbered from 1 to 3 on Figure 7. Line 1 was equipped with a CMOS camera for the adjustment of the laser beam line with respect to the slit. This alignment is done at low power before the heating experiments. Another line on the opposite side was also equipped with a similar camera for alignment. Line 2 was equipped with a monochromatic pyrometer operating at $1.27 \mu\text{m}$, this wavelength corresponds to the X-point region of W where emissivity does not vary as a function of temperature (Cagran et al, 2005). It has been used to measure the surface temperature of the hood during the experiments. On line 3 a thermal camera has been used to observe the thermal gradients on the hood surface.

An upper viewport gives access to the crucible cover and the sample through the opening (line 4). During the experiments this line has been equipped with either a pyrometer pointing on the cover for temperature measurements, a thermal camera to observe the thermal gradients on the surface, or a camera to observe the sample through the opening.

IV.c. Temperature measurements

The evaluation of the sample temperature is a critical point in the experiment. Optical pyrometry could be used to measure the temperature of the sample through the opening but this option was not selected because of the final application on irradiated fuels and experience on the current MERARG system: gas release, fragmentation of the sample or unknown emissivity implies too much uncertainty on the temperature. Alternatively, the crucible was equipped with a thermocouple type C inserted in the internal chamber described in Figure 2. For the hot cell application, the temperature measured by the thermocouple will be used for the laser power regulation through a feedback loop, as it is the case on the current MERARG system for adjustment of the power of the HF generator (Pontillon, 2009). It

is then necessary to have a good knowledge of the relation between this measured temperature and the sample temperature, which is not directly accessible. For that we rely on the numerical simulations and the different temperature measurements available that we summarize on Figure 8. The investigation of the correlation between these different measurements and the sample temperature is carried out in the next section.

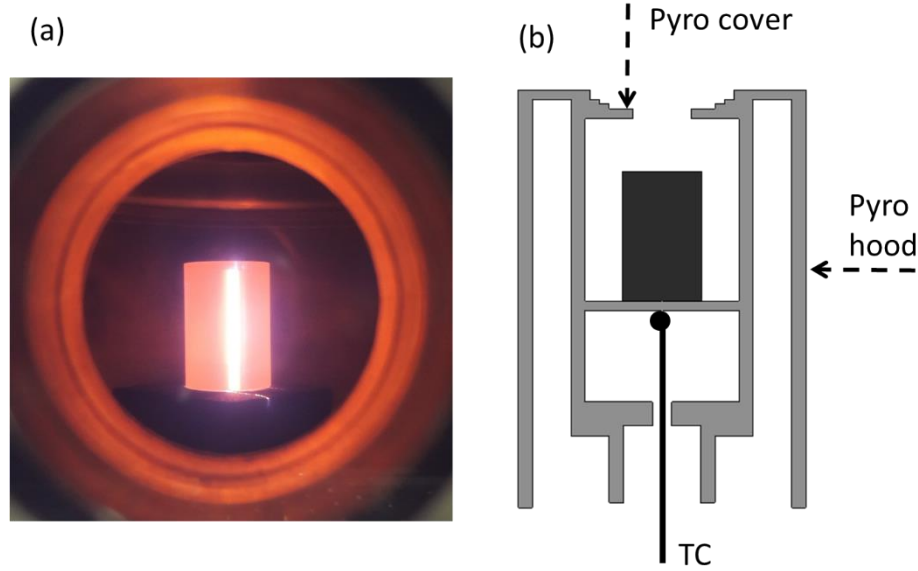


Figure 8: Temperature measurements on the hood/crucible assembly. (a) Observation of the assembly during a laser heating sequence through one of the viewport. One slit entrance is facing the viewport. (b) Location of the different temperature measurements during the experiments: two pyrometric measurements and one thermocouple measurement.

Uncertainty analysis of the temperature measurements with the used instruments (pyrometers and thermocouple) applied to Tungsten can be found in reference (Minissale et al, 2020). The maximum uncertainty is related to pyrometric measurements and is related on the one hand on the sensor (given as $\pm 2\%$ of the temperature reading by the manufacturer) and on the other hand on the uncertainty on emissivity of Tungsten material used in these experiments. With a conservative value of 10% uncertainty on the emissivity the related uncertainty on the temperature is $10-3T$, with T the temperature in Kelvin. For instance, at 2000 K it corresponds to 2%. The total uncertainty in this case can then be estimated to 4%.

V. Results and Discussion

V.a. Temperature calibration

We report firstly on the methodology that has been developed and the calibration experiments that have been conducted in order to link the sample temperature to the 3 external temperature measurements (the 2 pyrometers and the thermocouple described in Figure 8). For calibration purpose we have used the thermal fuse method: a material with a well-known melting point is heated in the crucible with in situ observation so that when fusion occurs the temperature is known. We have worked with Copper, with a melting point of 961°C, and silver, with a melting point of 1085°C. Filaments of these materials were inserted in a sample mock-up made of alumina, that was observed through the crucible opening during the heating experiments. The laser power was then slowly increased, to obtain heating ramps of typically 1°C/s, up to observation of melting of the fuse material. An example of such a heating sequence and temperature measurements is described in Figure 9.

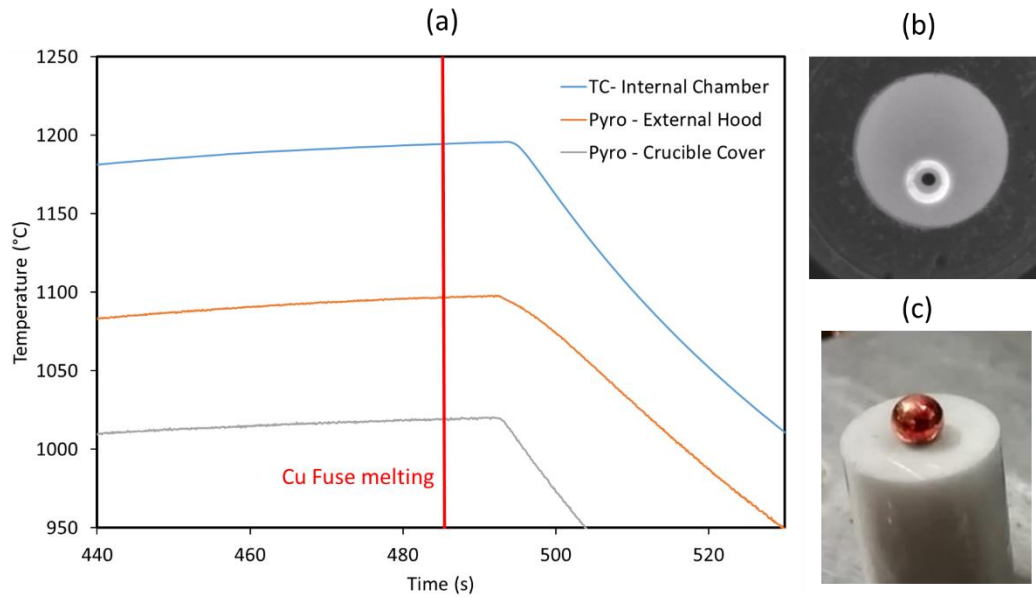


Figure 9: Results of a calibration experiment conducted with thermal fuses. (a) The temperature measured by the different instruments, at positions given on Figure 8. At time 485 s after the start of the laser heating sequence, melting of the copper fuse is observed with the in situ observation system. (b) in situ observation of melting of the copper fuse. (c) The sample after removal from the crucible: the fused copper is visible at the top of the alumina holder.

The experimental results obtained have been compared to simulations performed with the finite element model based on coupled optical/thermal simulations described previously. The model was used to obtain the temperature distribution in the hood/crucible assembly and at the positions of the measurements. This approach is intended to give the correlation factor between the available measurements during an experiment, and the real temperature of the sample that cannot be directly monitored. Figure 10 reports on an example of such a temperature distribution, calculated for experimental conditions, with the location of the 3 measurements (pyrometers and thermocouple) indicated, and the simulated / experimental temperature reported at these 3 locations.

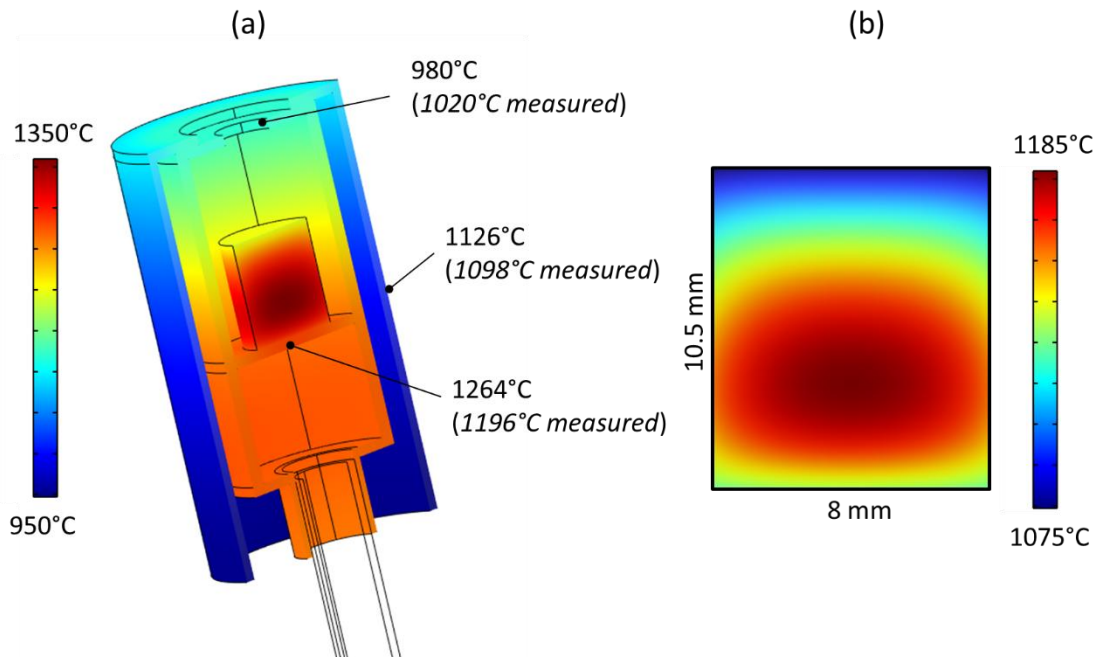


Figure 10: (a) Simulation of the temperature distribution in the crucible/hood assembly for an input power of 230 W after reaching the stating state regime. The calculated temperatures are reported on the 3 measurement locations in the experiment: crucible cover, external hood, and internal chamber at the location of the thermocouple. (b) Temperature distribution in the core of pellet sample.

The calculated values are consistent with the experiment, with however some deviations. These deviations however lie below the 5% range in the reported example on Figure 10, and in the other investigated case with Silver as fused material. On this basis, we can then relate the temperature distribution in the assembly and sample to the thermocouple measurement through the simulation. The TC measurement is chosen as the reference since it is used in the feedback control loop of the laser power for reasons exposed previously and it cannot be affected by changes of emissivity or optical attenuation due to window contamination as the pyrometer could be in future hot cell experiments. If we now look at the relation between the TC temperature and the sample temperature, which is the one of interest, the calibration experiments on fuse materials have led to a temperature ratio of 1.1: fuse of silver (melting point of 961°C) is observed for TC temperature of 1052°C and fuse of copper (1085°C) is observed for TC temperature of 1194°C. Obtaining this temperature ratio concludes the thermal qualification phase of the system. One can notice that a more complete approach consists of using a second thermocouple inserted in the core of a pellet instead of a fuse material. Both approaches are used as standard procedures on the MERARG system [Vidal et al, 2020].

V.b. Laser controlled heating of UO₂ target

From the previously described calibration measurements, it was possible to obtain a correlation coefficient between the sample temperature and the TC temperature. The objective of experiments is then to obtain smooth and well controlled heating ramps, as well as stable temperature plateau. The qualification of the temperature regulation system was done with dedicated experiment with a UO₂ pellet in the crucible and with one of the pyrometer pointing at the surface of the UO₂ pellet through the opening in the crucible to monitor its temperature. An example of a regulated temperature sequence is given in Figure 11. This particular sequence corresponds for the UO₂ sample to a targeted

ramp of 5°C/s from ambient to 1300°C, followed by a temperature plateau for few minutes. As shown on this figure the heating rate corresponds to the setting rate and the temperature plateau is stable within $\pm 1^\circ\text{C}$ with a minimal overshoot of less than 10°C, which corresponds to less than 1% of the setting point.

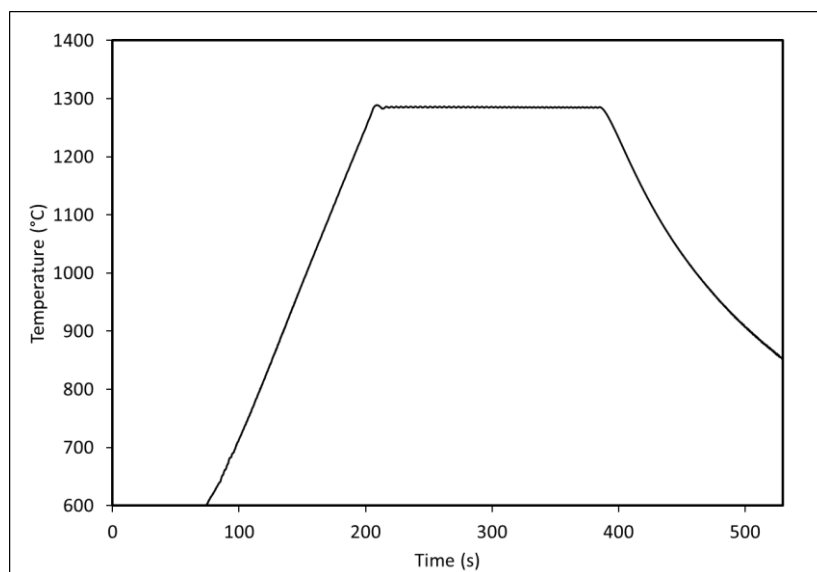


Figure 11: Laser heating sequence with active regulation. Reported is the temperature measured at the surface of the UO_2 sample in the crucible. This measurement is done with a pyrometer through the opening in the crucible.

At this point, maximum temperature ramps up to 30°C/s have been achieved (Figure 12). Higher heating rates can be theoretically achieved, the limitation at this point being the available laser power on the experimental set-up (1 kW).

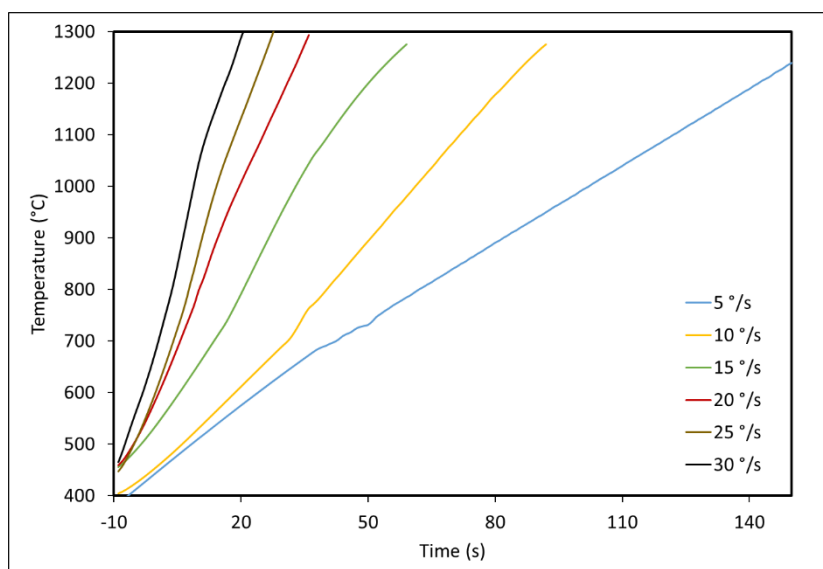


Figure 12: Different obtained heating ramps with described system. The measurements are done with a pyrometer through the opening in the crucible.

Finally, these experiments have been conducted under vacuum as the goal was to validate the concept of these experiments. If these experiments were to be conducted on irradiated fuel, a sweeping gas would be used to carry out the released gaseous fission products towards the online measurement loop. The presence of this sweeping gas would induce heat losses through convective heat exchange and should be taken into account in the simulations if one wants to accurately predicts the thermal response of the experiment for a given laser power.

Conclusion

Annealing tests are of utmost importance in nuclear fuel research particularly to study thermophysical properties of the material, micro structure evolution or the released gas as a function of temperature. As an alternative to conventional furnace or induction annealing, we have introduced and demonstrated in this work a laser-heating device that can drive nuclear fuel pellets at high temperature in well-controlled conditions. The current system can be used to heat nuclear fuel pellets up to 1500°C at a maximum heating rate of 30°C/s with the use of two 500 W lasers. The system is however scalable to higher heating rates or higher temperatures since few kW laser systems are now easily available. The perspective of our work is now to integrate this technique on the MERARG platform in order to be able to investigate nuclear fuel behavior under various conditions, by using the flexibility of the laser heating technique.

Supplementary Material

The details of the COMSOL simulations are provided as a supplementary material document.

Author's contributions

C. Cifuentes Quintal: Investigation, Software; **M. Reymond:** Formal Analysis, Investigation, Software, Writing/Original Draft Preparation ; **F. Fiorito:** Resources; **F. Martin:** Resources ; **M. Pontillon:** Resources ; **J.C. Richaud:** Resources ; **T. Doualle:** Formal Analysis, Investigation, Methodology, Software, Writing/Review & Editing ; **Y. Pontillon:** Conceptualization, Investigation, Methodology, Project Administration, Supervision, Writing/Review & Editing ; **L. Gallais:** Conceptualization, Methodology, Supervision, Visualization, Writing/Original Draft Preparation.

Acknowledgments

This work was conducted in the framework of the MATLASE chair, a joint research and teaching program between Ecole Centrale Méditerranée et CEA Cadarache.

The authors wish to thank EDF and Framatome for supporting this work in the frame of Tripartite Institute (CEA/EDF/FRA).

Data availability statement

The data that support the findings of this study are available from the corresponding author upon reasonable request.

References

- Cagran, C. ; Pottlacher, M. G. ; Rink, M. ; Bauer, W., Spectral emissivities and emissivity x-points of pure molybdenum and tungsten,” Int. J. Thermophys. 26, 1001 (2005).
- Colle, J.-Y. ; Capone, F., Very high temperature laser heated furnace for Knudsen cell mass spectrometry. 79, 55105–0 (2008).

Davis, J.W. ; Smith, P.D., ITER material properties handbook, J. Nucl. Mater. 233–237, 1593-1596 (1996).

Fink, J.K., Thermophysical properties of uranium dioxide, J. Nucl. Mater. 279, 1–18 (1999)

Gallais, L. ; Vidal, T. ; Lescoeur, E. ; Pontillon, Y. ; Rullier, J.-L., High power continuous wave laser heating of graphite in a high temperature range up to 3800 K, J. Appl. Phys. 129, 043102 (2021).

Horlait, D., Faure, R., Thomas, B. A., Devert, N., Amany, M.-L., Carlo, G., Gilabert, E., A new thermo-desorption laser-heating setup for studying noble gas diffusion and release from materials at high temperatures. Review of Scientific Instruments 92, 124102 (2021).

Manara, D.; Sheindlin, M.; Heinz, W.; Ronchi, C. New techniques for high-temperature melting measurements in volatile refractory materials via laser surface heating. Review of Scientific Instruments, 79, 113901 (2008)

Menegon, P., Desgranges, L., Pontillon, Y., Poulesquen, A., Evidence of two gas release kinetics during the oxidation of an irradiated PWR UO₂ fuel. J. Nucl. Mater. 378, 1 (2008).

Minissale, M. ; Pardanaud, C. ; Bisson, R. ; Gallais, L., The temperature dependence of optical properties of tungsten in the visible and near-infrared domains: an experimental and theoretical study, J. Phys. D: Appl. Phys. 50, 455601 (2017).

Minissale, M. ; Durif, I. ; Huret, P. ; Vidal, T. ; Faucheux, J. ; Lenci, M. ; Mondon, M. ; Kermouche, G. ; Pontillon, Y. ; Grisolia, C. ; Richou, M. ; Gallais, L., A high power laser facility to conduct annealing tests at high temperature, Rev. Sci. Instrum. 91, 035102 (2020).

Pontillon, Y., Desgranges, L., Poulesquen, A., ADAGIO technique: from UO₂ fuels to MOX fuels. J. Nucl. Mater. 385, 137 (2009).

Noirot, J., Pontillon, Y., Yagnik, S., Turnbull, J., Tverberg, T., Fission gas release behaviour of a 103 gwd/t(hm) fuel disc during a 1200 degrees C annealing test. J. Nucl. Mater. 446, 163 (2014).

Ravel, S., Emetin, G., Muller, E., Caillot, L., Pagas inventories: results obtained using the ADAGIO facility, Proceedings of the Fission Gas Behaviour in Water Reactor Fuels, 347, Nuclear Science OECD NEA, OECD, Cadarache, France (2000)

Reymond, M., Sercombe, J., Gallais, L., Doualle, T., Pontillon, Y., ‘Thermo-mechanical simulations of laser heating experiments on UO₂’, Journal of Nuclear Materials 557, 153220 (2021)

Vidal, T., Gallais, L., Burla, R., Martin, F., Capdevila, H., Clément, S., Pontillon, Y., ‘Optical system for real-time monitoring of nuclear fuel pellets at high temperature’, Nuclear Engineering and Design 357, 110383 (2020).

Vidal, T., Gallais, L., Faucheux, J., Capdevila, H., Sercombe, J., Pontillon, Y., ‘Simulation of reactivity initiated accident thermal transients on nuclear fuels with laser remote heating’, J. Nucl. Mater. 530, 151944 (2020)

Weber, J. K. R., Tamalonis, A., Benmore, C. J., Alderman, O. L. G., Sendelbach, S., Hebden, A., Williamson, M. A., ‘Aerodynamic levitator for in situ x-ray structure measurements on high temperature and molten nuclear fuel materials’, Rev. Sci. Instrum. 87, 073902 (2016)